GEOPHYSICS, VOL. 61, NO. 1 (JANUARY-FEBRUARY 1996); P. 288–293, 5 FIGS., 2 TABLES.

Short Note

Elasticity of partially saturated frozen sand

Maureen Jacoby*, Jack Dvorkin‡, and Xingzhou Liu**

INTRODUCTION

Seasonal thawing and freezing of near-surface sediments significantly affect the interpretation of seismic reflection surveys and vertical seismic profiling, as well as activity on the surface. Permafrost covers much of the Earth's colder regions and is also subject to periodic thawing and freezing. The significance of the regions with large seasonal temperature variations for exploration and engineering activities makes understanding the elasticity of frozen ground an important practical and scientific goal.

Previous theoretical and experimental studies of seismic velocities in frozen rocks (e.g., Timur, 1968) showed that *P*-wave velocity in fully water-saturated rocks increases with decreasing temperature, whereas it is almost independent of temperature in dry rocks. As temperature decreases, saturated rocks become (given enough time) completely frozen, and velocity reaches its constant (terminal) value. A theoretical scheme for estimating both *P*- and *S*-wave velocities in saturated freezing rocks has been proposed by Zimmerman and King (1986); the method accurately predicted the experimental data.

In this study, we are concerned with velocities in partially saturated unconsolidated sands. Our experiments show that in hydrophilic granular materials, velocities may be close to their full-saturation terminal values at saturations as small as 10–15%. The reason for this strong velocity increase from the dry state is the cementing action of ice that forms pendular rings at the grain contacts. This freezing effect is a special case of a more general phenomenon: even small amounts of relatively soft cement, if placed at the grain contacts, act to dramatically increase the stiffness of the aggregate.

By applying the Dvorkin et al. (1994) intergranular cementation theory, we accurately predict the measured experimental values. These accurate predictions cannot be achieved by effective medium theories that do not take into consideration the specific location of the cement—at the grain contacts.

EXPERIMENTS

The laboratory apparatus includes a 76-cm-long, 7.6-cm diameter Plexiglas holder filled with the dry-matrix material (0.7-mm diameter, well-sorted glass beads or Ottawa sand with average grain size 0.3 mm). *P*- and *S*-wave velocities are measured within the holder using transmitter and receiver transducers (both 2.5 MHz central frequency) placed 1.52 cm apart. The transducers are held within a rigid plastic frame, which is lowered into the Plexiglas tube by the cables. The holder is seated on a metal base with drainage holes.

The matrix materials were saturated by suctioning degassed water up the tube through the holes in the base. This technique allowed air to escape and prevented air bubbles from lodging in the matrix. Partial saturation was achieved by draining the fully saturated matrix materials. The amounts of water held by capillary forces between the grains were uniform along the upper part of the holder and accounted for 13.1 and 13.5% saturation in glass beads and Ottawa sand, respectively. Both matrix materials appeared to be hydrophilic—water formed pendular rings around grain contacts.

P- and *S*-wave velocities were measured in the samples (dry, saturated, and partially saturated) after they spent a day in a freezer at about −20°C (to ensure the complete freezing of water). The results of these measurements, as well as the experimental values for dry-matrix porosity and ice saturation of the pore space, are summarized in Table 1.

The measured ultrasonic velocities are plotted versus ice saturation in Figure 1. At zero ice saturation, both *P*- and *S*-wave velocities are zero since no confining pressure is applied to the samples. A dramatic increase in the velocities is apparent as ice saturation increases from zero to about 13%.

Manuscript received by the Editor June 6, 1994; revised manuscript received March 13, 1995.
*Formerly Dept. of Geophysics, Stanford University, Stanford, CA 94305-2215; presently Archibald Mining and Minerals Inc., 1685 Baltimore Pike, Gettysburg, PA 17325.
‡Dept. of Geophysics, Stanford University, Stanford, CA 94305-2215.
**Formerly Dept. of Geophysics, Stanford University, Stanford, CA 94305-2215; presently Western Atlas International, P.O. Box 1407, Houston, TX 77251-1407.

This increase is much larger than that occurring between low and full saturation.

EFFECT OF CEMENTATION

The observed strong velocity increase at low ice saturations is apparently caused by the cementing effect of frozen pendular rings. Indeed, the theoretical and experimental results in Dvorkin et al. (1994) show that even small amounts of relatively soft cement, if placed at grain contacts, dramatically increase the stiffness of an aggregate. We applied the cementation theory of Dvorkin et al. (1994) to calculate the effective elastic moduli of ice-cemented glass beads and Ottawa sand (the algorithm is given in the Appendix). Both aggregates were modeled as assemblies of randomly packed identical elastic spheres (glass and quartz) with elastic cement (ice) at the contacts. The material properties used in these calculations are summarized in Table 2.

All densities, as well as *P*- and *S*-wave velocities in ice, were measured by the authors. *P*- and *S*-wave velocities in glass were taken from Berge et al. (1993). The velocities in Ottawa sand grains were obtained indirectly by using Hill's (1952) average to calculate the effective moduli of the fully-saturated sand-ice mixture and adjusting those of the grains to match the experimental results. The equations for calculating an effective modulus (M_{Hill}) are

$$M_{\text{Hill}} = (M_V + M_R)/2,\ M_V = (1-\phi_0)M_{\text{Sand}} + \phi_0 M_{\text{Ice}},$$
$$1/M_R = (1-\phi_0)/M_{\text{Sand}} + \phi_0/M_{\text{Ice}}, \quad (1)$$

where M_{Sand} and M_{Ice} are the moduli of the sand grain material and ice, respectively, and ϕ_0 is the porosity of a dry matrix. These equations can be used to calculate bulk (K), shear (G), and *P*-wave (M) moduli. The latter is related to *P*-wave velocity as $M = \rho V_P^2$, where ρ is density.

The values thus obtained for V_P and V_S in the sand-grain material are about 86% to 89% those in pure quartz—6050 m/s and 4090 m/s, respectively (Carmichael, 1989). Nevertheless, we decided to use the calculated values because the elastic moduli of sand grains may be lower than those of pure quartz because of microcracks.

Our theoretical calculations are compared with the experimental values of the *P*-wave and shear moduli in Figures 2 and 3. The moduli are plotted versus the porosity ϕ of an aggregate—$\phi = \phi_0(1 - S)$, where S is the volumetric ice saturation. The theoretical curves begin at porosity 0.2 because the cementation theory can be used only for small amounts of intergranular cement. We observe a good match between the experimental data and the theoretical predictions for glass beads. In Ottawa sand, the accuracy of the theoretical prediction is still satisfactory (the error is 15%) for the *P*-wave modulus, whereas for the shear modulus the error reaches 34%. Notice, that for V_P and V_S, these errors become 7% and 16%, respectively. This difference between the predicted and the measured values is most likely a result of the angularity of the sand grains: the cemented contact area between angular grains is smaller than that between two spheres (for the same amount of cement).

The second reason for the disparity may be a more uniform distribution of ice on the surface of the Ottawa sand grains. In this case only part of the ice—the intersection of ice shells around the grains—forms contact cement. We model the latter situation by representing Ottawa sand as a pack of identical spheres with ice uniformly distributed on their surfaces. This model gives a low-bound estimate for the effective elastic moduli. This lower bound is shown in Figure 3 for the effective shear modulus. The span between the upper and lower bounds is fairly large for elastic moduli. However, this span becomes much smaller for *P*- and *S*-wave velocities (Figure 4). Therefore, our theoretical bounds can be used for practical estimates of velocities in frozen partially saturated sands.

Table 1. Results of experimental measurements.

Matrix-cement	Dry-matrix porosity	Ice saturation	V_P (m/s)	V_S (m/s)
Glass-ice	0.4066	1.0	4583.	2492.
Ottawa sand-ice	0.3875	1.0	4480.	2730.
Glass-ice	0.4066	0.131	3418.	2100.
Ottawa sand-ice	0.3875	0.135	3040.	1900.
Glass-ice	0.4066	0.0	0.	0.
Ottawa sand-ice	0.3875	0.0	0.	0.

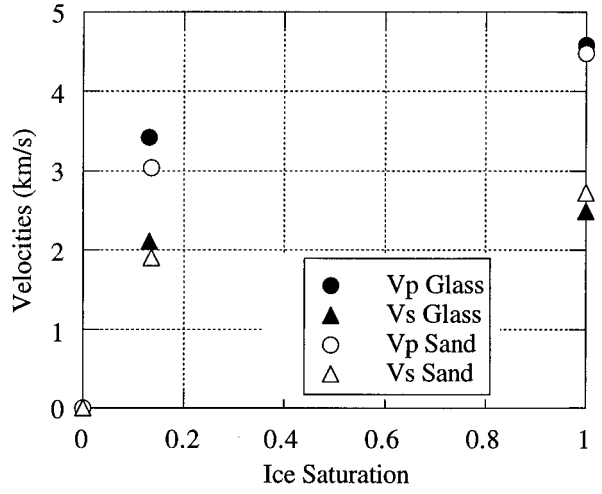

FIG. 1. Velocities in uncompacted frozen glass beads and Ottawa sand versus ice saturation.

CRITICAL POROSITY AND EFFECTIVE MEDIUM CALCULATIONS

Advanced effective medium theories, such as the self-consistent approximation (e.g., Berryman, 1980; Berge et al., 1993), have been successfully used for modeling the effective

Table 2. Material properties of ice, glass, and sand grains.

Substance	V_P (m/s)	V_S (m/s)	Density (kg/m^3)
Ice	3840.	1980.	900.
Glass	5860.	3480.	2505.
Sand grains	5372.	3517.	2668.

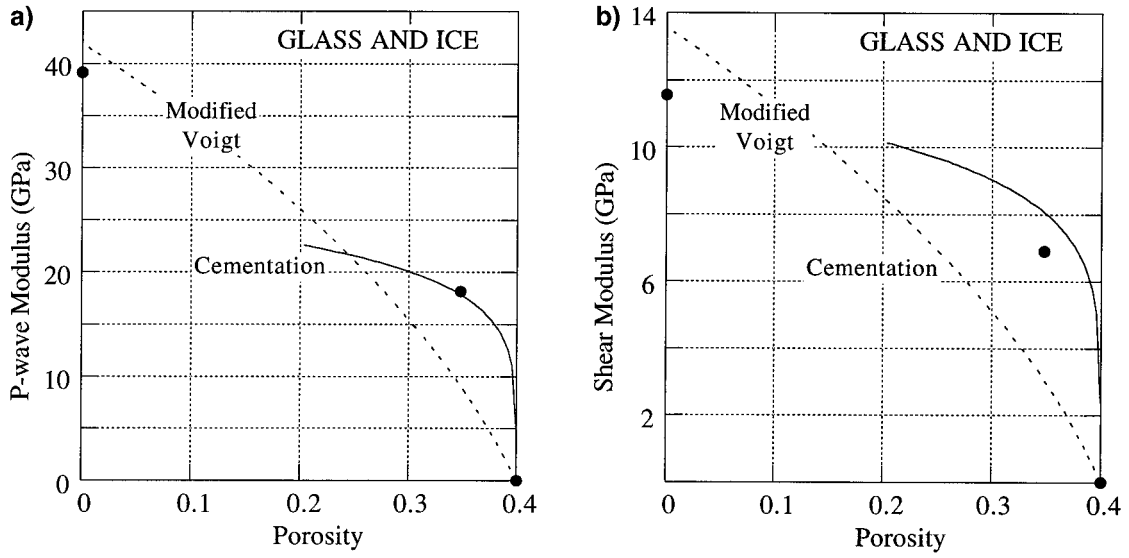

FIG. 2. *P*-wave (a) and shear (b) moduli in ice-cemented glass beads. Circles—experiments, solid lines—the cementation theory, dashed line—modified Voigt average. The porosity is that of the frozen sample, including ice as part of the matrix. The zero porosity point is from the fully-saturated case, and the 0.4 porosity point is from the dry case, with the other point representing partial saturation.

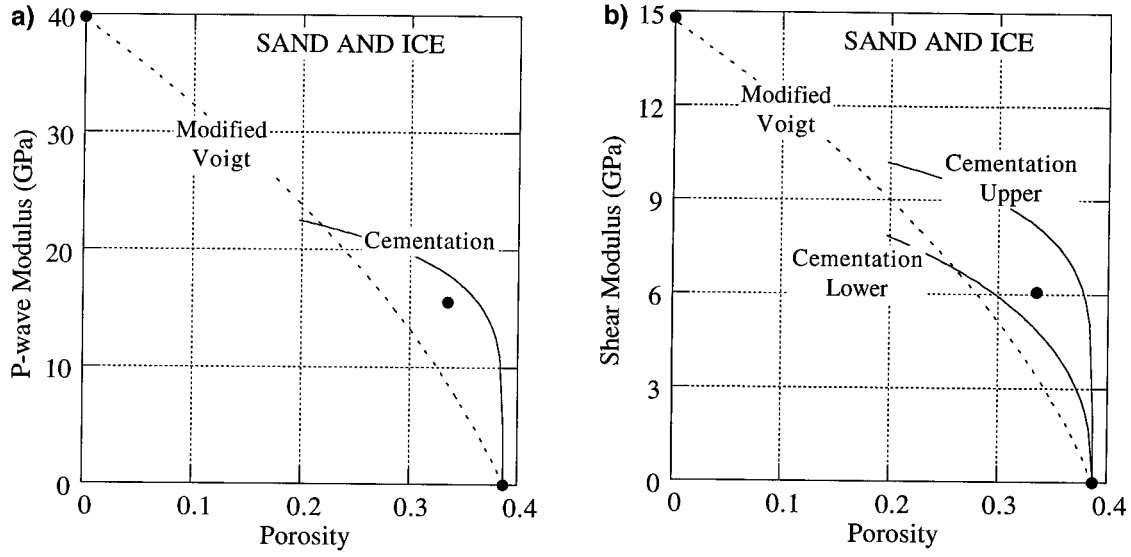

FIG. 3. *P*-wave (a) and shear (b) moduli in ice-cemented Ottawa sand. Circles—experiments, solid lines—the cementation theory, dashed line—modified Voigt average. Porosity is defined in the caption of Figure 2.

properties of composites. However, these theories do not make explicit use of the fact that at zero confining pressure in dry unconsolidated, uncemented granular materials, elastic waves do not propagate, and elastic moduli are zero. In this case, the elastic modulus curves (in the modulus-porosity plane) have to intercept the porosity axis at a certain terminal (critical) porosity (ϕ_c). In sands, this critical porosity is about 0.38—the value close to the porosity of randomly packed identical spheres. Generally, in effective medium theories, this intercept occurs at values higher than the realistic ϕ_c value for a given aggregate (e.g., Berge et al., 1993). Nur et al. (1991) propose that this critical porosity value is a natural physical boundary for using effective medium relations in sandstones and sands. They show that one can arrive at accurate estimates for velocities in sandstones by using a heuristic, modified Voigt average formula

$$M_{\text{Effective}} = M_{\text{Solid}}\left(1 - \frac{\phi}{\phi_c}\right), \qquad (2)$$

where M_{Solid} may be the solid phase's bulk, shear, or *P*-wave modulus. The solid phase moduli have to be calculated from those of mineral components by using weighted averages, such as that of Hill (1952).

We now apply equation (2) to estimating the effective modulus of ice-cemented glass beads and Ottawa sand by assuming that the grains and the ice form a single solid phase whose effective moduli can be calculated from Hill's average—equation (1). The latter assumption is supported by the fact that Hill's average gives fairly accurate estimates to the effective moduli of frozen glass beads at full ice saturation.

The results of these calculations are given in Figures 2 and 3. In many rocks, the modified Voigt average formula can accurately predict the moduli at small and medium porosities (Nur et al., 1991). We show here that it may fail to predict the dramatic increase of these moduli that occurs as porosity reduces slightly from its initial (dry) value. The reason is that this average does not take into account the special arrangement of the ice cement among grains—directly at their contacts. Practically, this arrangement is relevant to the case of frozen partially saturated sands.

Zimmerman and King (1985) give an important example of applying an effective medium theory (Kuster and Toksöz, 1974) to modeling velocities in fully saturated freezing sands, shales, and silts. The theoretical scheme is: first the elastic moduli of the ice-air mixture (the ice is the matrix) are computed by using the Kuster-Toksöz formula for spherical inclusions. Then the effective moduli of the frozen aggregate are computed by assuming that the ice-air mixture is the matrix and the grains are spherical inclusions. By comparing these predictions with experimental data, Zimmerman and King show that this theoretical approach gives accurate estimates to velocities in permafrost. We applied the recommended theoretical scheme to calculating *P*-wave and shear moduli for partially saturated frozen glass beads (Figure 5).

The Kuster-Toksöz (1974) scheme gives adequate estimates for the moduli at full saturation. But again, it fails to mimic the high-porosity elastic properties of partially saturated frozen granular materials. A likely reason is that in fully saturated rocks ice forms first in the larger pore spaces, and then in progressively smaller ones (Williams and Smith, 1989). However, in partially saturated hydrophilic materials where water forms pendular rings, ice forms at grain contacts and acts as strong cement. In this case, the cementation theory in Dvorkin et al. (1994) is apparently more appropriate.

CONCLUSIONS

In hydrophilic partially saturated frozen sands, ice acts as intergranular cement by forming pendular rings around grain contacts. This arrangement leads to strong *P*- and *S*-wave velocity increase between dry and partially saturated frozen samples at low saturations. This velocity increase is much larger than that occurring between low and full saturation.

The experimental results can be accurately modeled by the theory of cementation that explicitly takes into account the special position of intergranular cement at grain contacts. The effective medium theories, while giving accurate estimates for

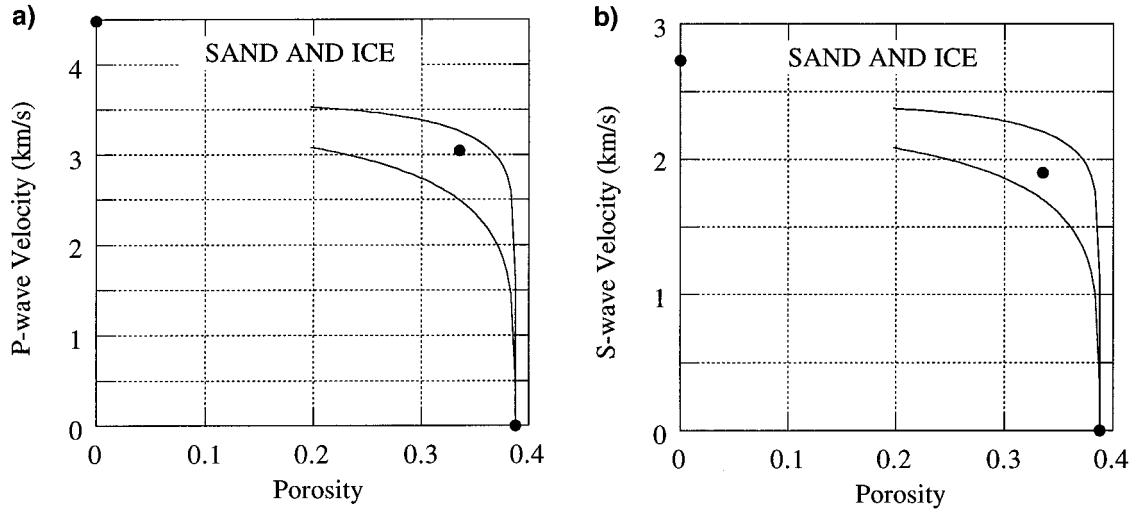

FIG. 4. *P*- (a) and *S*-wave (b) velocities in ice-cemented Ottawa sand. Circles—experiments, solid lines—the cementation theory, upper and lower bounds.

velocities at high ice saturation, fail to predict the observed dramatic velocity increase that occurs as small amounts of ice are added to grain contacts.

By assuming two geometrical schemes of ice distribution in the pore space (one in which ice is concentrated at the grain contacts, and another in which ice is uniformly distributed on the grain surface), the theory of cementation provides fairly narrow upper- and lower-bound estimates for *P*- and *S*-wave velocities in partially saturated frozen sands. These bounds can be used in practical estimates of the elastic properties of permafrost.

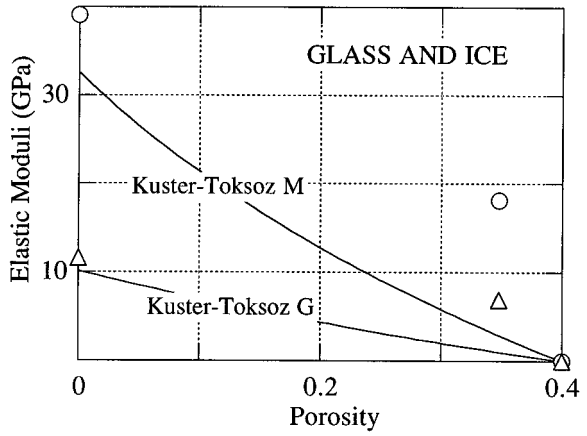

FIG. 5. Kuster-Toksöz-Zimmerman estimates for elastic *P*-wave (*M*) and shear (*G*) moduli in frozen glass beads. Circles—experimental points for *M*, triangles—experimental points for *G*.

ACKNOWLEDGMENTS

The study was supported by the U.S. Air Force Office of Scientific Research, Project 2302C and by Stanford Rock Physics Laboratory.

REFERENCES

Berge, P. A., Berryman, J. G., and Bonner, B. P., 1993, Influence of microstructure on rock elastic properties: Geophys. Res. Lett., **20**, 2619–2622.

Berryman, J. G., 1980, Long-wavelength propagation in composite elastic media. I. Spherical inclusions: J. Acoust. Soc. Am., **68**, 1809–1819.

Carmichael, R. S., 1989, Practical handbook of physical properties of rocks and minerals: CRC Press.

Delves, L. M. and Mohamed, J. L., 1985, Computational methods for integral equations: Cambridge Univ. Press.

Dvorkin, J., Yin, H., and Nur, A., 1994, Effective properties of cemented granular materials: Mechanics of Materials, **18**, 351–366.

Hill, R., 1952, The elastic behavior of crystalline aggregate: Proc. Phys. Soc. London, **A65**, 349–354.

Kuster, G. T., and Toksöz, M. N., 1974, Velocity and attenuation of seismic waves in two-phase media. Part 1. Theoretical formulations: Geophysics, **39**, 587–606.

Nur, A., Marion, D., and Yin, H., 1991, Wave velocities in sediments, in Hovem, J. M., Richardson, M. D., and Stoll, R. D., Eds., Shear waves in marine sediments: Kluwer Academic Publ.

Timur, A., 1968, Velocity of compressional waves in frozen soils at permafrost temperatures: Geophysics, **33**, 584–595.

Williams, P. J., and Smith, M. W., 1989, The frozen earth: Cambridge Univ. Press.

Zimmerman, R. W., and King, M. S., 1986, The effect of the extent of freezing on seismic velocities in unconsolidated permafrost: Geophysics, **51**, 1285–1290.

APPENDIX

APPLYING THEORY OF CEMENTATION

1) Find the ratio of the cement layer radius to the grain radius α as

$$\alpha = \left[\frac{16}{3}\frac{S_{ice}\phi_0}{N_c(1-\phi_0)}\right]^{0.25} \qquad \text{(A-1)}$$

if all cement is concentrated at the grain contacts, and as

$$\alpha = \sqrt{\frac{2}{3}\frac{S_{ice}\phi_0}{1-\phi_0}} \qquad \text{(A-2)}$$

if cement is evenly distributed on the grain surface. These two formulas give the upper- and lower-bound estimates, respectively. Here S_{ice} is ice saturation of the pore space, ϕ_0 is dry-rock porosity, and N_c is the average number of contacts per grain (about 8.5 for unconsolidated high-porosity sands).

2) Find an as yet unknown function $H(t)$ from the integral equation

$$\Delta_0 + H(t) = -2\Lambda \int_0^{\pi} d\varphi \int_0^{t\cos\varphi + \sqrt{\alpha^2 - t^2\sin^2\varphi}} \frac{H(\sqrt{t^2+s^2-2ts\cos\varphi})}{t^2+s^2-2ts\cos\varphi}\, ds, \qquad \text{(A-3)}$$

where Δ_0 is an arbitrarily chosen nonzero constant, and

$$\Lambda = \frac{2G_{Ice}}{\pi G_{Grain}}\frac{(1-\nu_{Grain})(1-\nu_{Ice})}{1-2\nu_{Ice}}, \qquad \text{(A-4)}$$

where G is shear modulus, and ν is Poisson's ratio.

3) Calculate integral

$$k = 2\int_0^{\alpha}\frac{H(t)\,dt}{t}. \qquad \text{(A-5)}$$

4) Calculate the effective bulk modulus of the frozen grains from

$$K_{eff} = \frac{G_{Ice}(1-\nu_{Ice})}{1-2\nu_{Ice}}\frac{N_c(1-\phi_0)}{3}\left(-\frac{k}{\Delta_0}\right). \qquad \text{(A-6)}$$

5) Find an as yet unknown function $H_1(t)$ from the integral equation

$$\Delta_0 + H_1(t) = -2\Lambda_s \int_0^{\pi} d\varphi \int_0^{t\cos\varphi + \sqrt{\alpha^2 - t^2\sin^2\varphi}} \frac{H_1(\sqrt{t^2+s^2-2ts\cos\varphi})(1-\nu\sin^2\varphi)}{t^2+s^2-2ts\cos\varphi}\, ds, \qquad \text{(A-7)}$$

where

$$\Lambda_s = \frac{G_{\text{Ice}}}{\pi G_{\text{Grain}}}. \quad \text{(A-8)}$$

6) Calculate integral

$$k_1 = 2\int_0^{\alpha} \frac{H_1(t)\,dt}{t}. \quad \text{(A-9)}$$

7) Calculate the effective shear modulus of the frozen grains from

$$G_{\text{eff}} = \frac{3}{5}K_{\text{eff}} + G_{\text{Ice}}\frac{3N_c(1-\phi_0)}{20}\left(-\frac{k_1}{\Delta_0}\right). \quad \text{(A-10)}$$

The integral equations allow for a straightforward numerical solution using the quadrature method (e.g., Delves and Mohamed, 1985). Upon request, the authors will provide a FORTRAN numerical code for calculating the effective moduli (direct requests to Jack Dvorkin).